Stationary and moving breathers in a simplified model of curved alpha--helix proteins

2002 J. Phys. A: Math. Gen. 35 8885

(http://iopscience.iop.org/0305-4470/35/42/301)

INSTITUTE OF PHYSICS PUBLISHING JOURNAL OF PHYSICS A: MATHEMATICAL AND GENERAL

J. Phys. A: Math. Gen. **35** (2002) 8885–8902 PII: S0305-4470(02)37793-X

Stationary and moving breathers in a simplified model of curved alpha–helix proteins

J F R Archilla[1], Yu B Gaididei[2], P L Christiansen[3] and J Cuevas[1]

[1] Nonlinear Physics Group of the University of Sevilla, Dep. Física Aplicada I, ETSI Informática, Avda. Reina Mercedes s/n, 41012 Sevilla, Spain
[2] Bogolyubov Institute for Theoretical Physics, 03143 Kiev, Ukraine
[3] Informatics and Mathematical Modelling, Technical University of Denmark , DK-2800 Lyngby, Denmark

E-mail: archilla@us.es

Received 7 June 2002
Published 8 October 2002
Online at stacks.iop.org/JPhysA/35/8885

Abstract

We study the existence, stability and movability of breathers in a model for alpha–helix proteins. This model basically consists of a chain of dipole moments parallel to it. The existence of localized linear modes means that the system has a characteristic frequency, which depends on the curvature of the chain. Hard breathers are stable, while soft breathers experience subharmonic instabilities that are preserved, whatever the localization. Moving breathers can travel across the bending point for small curvature and are reflected when it is increased. No trapping of breathers takes place.

PACS numbers: 63.20.Pw, 63.20.Ry, 66.90.+r, 87.10.+e

1. Introduction

In the last few years, quite a large amount of research has been carried out on localization due to the interplay of nonlinearity and geometry, either with the nonlinear Schrödinger equation [1, 2], FPU models [3–5], Klein–Gordon models [6, 7] or in DNA models [8, 9]. The objective has been to understand the role of the bending points in biomolecules; whether localized excitations can travel across them or not, and whether there are points where energy is stored and plays a biological function. The description of the biological systems is given by variables that represent internal or external degrees of freedom, which oscillate with time and are coupled by different potentials. A change of geometry can be felt by the system by different physical mechanisms, modelled correspondingly: interaction between nearest and next-nearest neighbours [4, 5]; potentials that depend on the angles [1] or long-range interaction due to the dipole–dipole coupling [2, 6, 7].

Simplifying, the effect of a curved chain can be described easily. For stationary excitations, the zone where the chain of oscillators is bent is inhomogeneous, bringing about the existence of localized linear modes which compete strongly with the nonlinear localized modes. For high coupling, the linear localization predominates; for low coupling the nonlinear localization is important. The transition from one regime to the other can be continuous or discontinuous as the parameters are changed or the curvature increases [7]. Moving excitations have to travel across this inhomogeneous zone. The excitation within the bending zone needs a different energy, which can be larger than in the straight system, therefore acting as a barrier. The excitation can be reflected, transmitted or trapped [10].

The alpha–helix protein is another molecule, for which it is interesting to investigate the role of bending in the existence, shape, properties and transport of localized excitations. The peptide groups have a dipole moment parallel to the chain and the amide-I excitations interact among them through acoustic phonons. The dipole–dipole interaction, which is described in detail in this paper, makes the system sensitive to the shape of the molecule. Apart from the interest of the biophysical problem in itself, it has a relevant feature from a more theoretical point of view; it is only necessary to take into account the nearest neighbours in order that the system can feel the bending of the chain. To our knowledge, the effects of curvature in such a system with dipoles parallel to the chain have not yet been described.

There are different excitations that can be considered, as solitons, envelope solitons and discrete breathers. Here, we focus our research on the latter. As is well known, discrete breathers are very localized oscillations that appear as a consequence of nonlinearity and discreteness [11–14]. They are, therefore, especially relevant in biomolecules when considering excitations that involve only a few units, far from the continuous limits. Although a relatively new field, stationary breathers are now well understood and research is presently focusing on the possible physical and biological consequences of their existence and in future technological applications, especially with Josephson junctions [15, 16]. The study of moving breathers is not such a mature field; there are techniques to obtain them but many questions remain unanswered [17, 18]. Perhaps the most important question is why they exist in some systems and not in others. New developments have been given in [19].

In this paper, we intend to complete previous works [6, 7, 10] on the properties of localization and transmission of energy in bent chains, described by Klein–Gordon models. The models in the references cited are inspired in DNA, with three main properties:

(i) there is a long-range interaction between dipole moments;
(ii) the dipole moments are perpendicular to the chain and to the plane of curvature;
(iii) the effect of curvature enters the model as a shortening of the distances between dipole moments.

The simplified alpha–helix model studied here, apart from its different physical origin, has the following differences:

(i) the only interactions considered are nearest-neighbour (note that the DNA models cited, without long-range interaction, would not feel at all the shape of the molecule);
(ii) the dipole moments are parallel to the chain and to the plane of curvature;
(iii) the bending of the chain appears in the model as a change in the angles between dipole moments and, therefore, in the interaction energy.

In spite of these differences, both models present very similar behaviour for both predominant stronger attractive and repulsive interaction. This suggests that they are generic on bent Klein–Gordon systems.

However, in this paper, we introduce a new point of view. Previous works have misinterpreted the mathematical property of the annihilation of breathers as the curvature

is increased. What happens is that the bending forces the breather at the bending point to choose some frequency, which depends weakly on its energy.

This phenomenon could, in principle, be tested experimentally. For example, the mean curvature of DNA depends on the solvent concentration, and the absorbtion of radiation by breathers at the bending points would appear at some characteristic frequencies that change with the solvent concentration. The presence of some harmonics of these frequencies would differentiate breathers from linear localized modes. Certainly, many technical problems should be expected, but we plan to perform this study with some experimental groups. Apparently, the more adequate molecule might be RNA due to its short persistence length.

The short section 6 deals with moving breathers. Its first objective is to check whether, in this model, breathers can move and are reflected by or transmitted through the bending point. The second objective is to confirm the trapping hypothesis introduced in [22] for a DNA model with an impurity. The role of an impurity is similar to a bending point in bringing about localized linear modes, which compete with the (nonlinear) breather localization. This hypothesis consists of the nonexistence of trapping for moving breathers when there exists a linear localized mode with a different tail profile, i.e. neighbouring sites in phase or with opposite phase (and, therefore, different frequency). There is no mathematical proof, but it is also confirmed in this paper in spite of the differences stated above.

2. Model description

We describe the position of each amino acid by $\boldsymbol{r}_n$, where n is an index. The distance between amino acids is supposed to be a constant a, i.e. $a = |\boldsymbol{r}_{n+1} - \boldsymbol{r}_n|$. The direction of the dipole moments are given by unit vectors $\boldsymbol{t}_n = \dfrac{(\boldsymbol{r}_{n+1} - \boldsymbol{r}_n)}{|\boldsymbol{r}_{n+1} - \boldsymbol{r}_n|}$ and the moments themselves are given by $\boldsymbol{p}_n = p_n \boldsymbol{t}_n$.

The Hamiltonian of the system, for which details have been given in appendix A, can be written as

$$H = \sum_n \frac{1}{2}\dot{u}_n^2 + \frac{1}{2}\omega_0^2 u_n^2 + \Psi(u_n) + \frac{1}{2}\varepsilon(u_{n+1} - u_n)^2 + \mu(\boldsymbol{t}_{n+1} - \boldsymbol{t}_n)^2 u_n u_{n+1} \tag{1}$$

with $\omega_0 = 1$. The on-site potential is given by $V(u_n) = \frac{1}{2}\omega_0^2 u_n^2 + \Psi(u_n)$, where $\Psi(u_n)$ is its nonlinear part.

The corresponding dynamical equations are

$$\ddot{u}_n + \omega_0^2 u_n + \Psi'(u_n) + \varepsilon(2u_n - u_{n+1} - u_{n-1}) + \mu((\boldsymbol{t}_{n+1} - \boldsymbol{t}_n)^2 u_{n+1} + (\boldsymbol{t}_{n-1} - \boldsymbol{t}_n)^2 u_{n-1}) = 0 \tag{2}$$

or, in a simplified notation,

$$f_n(u) \equiv \ddot{u}_n + \omega_0^2 u_n + \Psi'(u_n) + \varepsilon \sum_m C_{n,m} u_m + \mu \sum_m J_{n,m} u_m = 0 \tag{3}$$

with the obvious definition of the coupling matrices C and J. Note that C does not depend on the parameters while J depends only on the curvature κ.

Certainly, many different shapes can be considered. Here we focus as in previous papers on a parabola in two-dimensional space. The reason is that it is the simplest form to describe a bending point and it is an approximation of any curve in the neighbourhood of it. Other shapes considered in the literature, such as the hairpin geometry, although interesting in themselves, are not so adequate for our purposes because, for example, the latter is composed by three homogeneous regions (except if considering long-range interaction). Therefore, the vectors $\boldsymbol{r}_n$ have components (x_n, y_n) with $y_n = \frac{1}{2}\kappa x_n^2$, where κ is the curvature.

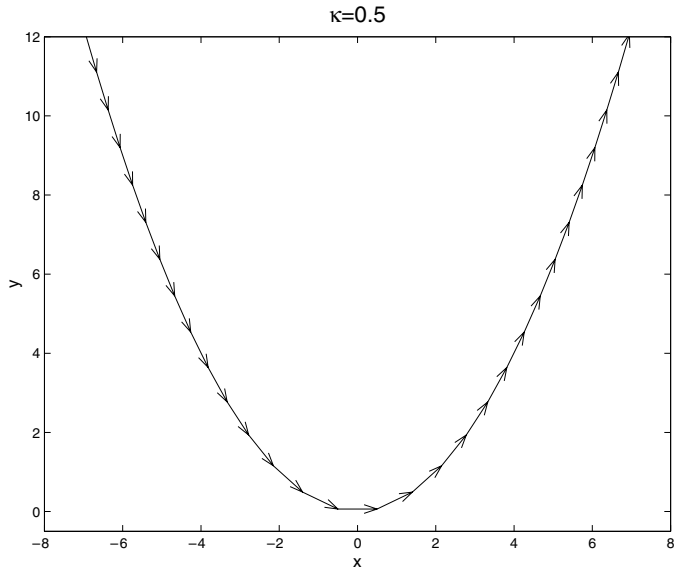

Figure 1. Schematic diagram of the model for curvature $\kappa = 0.5$.

A schematic diagram of the model is shown in figure 1.

In spite of having many dimensionless variables, there are still a few parameters in our problem: ε, which will be called the stacking coupling parameter; μ, the dipole coupling parameter; the curvature κ; and the breather frequency, which we represent by ω_b. The distance of ω_b from the phonon band is a measure of the degree of nonlinearity of the excitation. Generally speaking, the more nonlinear the excitation, the narrower it becomes. It is a daunting task to explore thoroughly the parameter space, but to obtain a general picture is a much more affordable task and this is what we intend here.

3. Linear modes

In bent systems there exist linear modes that are localized around the bending point. The first step is therefore to obtain the dependence of the linear spectrum on the parameters and to identify the most important ones. The linear modes are the solutions of equation (3) with $\Psi = 0$. We first obtain the dependence on the stacking parameter ε without dipole coupling or equivalently for a straight chain, i.e. either $\mu = 0$ or $(\boldsymbol{t}_{n+1} - \boldsymbol{t}_n) = 0, \forall n$ in equation (3). Figure 2 shows this spectrum dependence.

This a well-known spectrum, which we include here for comparison. Let us comment on three facts. Firstly, the spectrum is continuous. Secondly, the mode with the highest frequency consists of all oscillators vibrating with opposite phase with respect to the nearest neighbours. Thirdly, the mode with the lowest frequency consists of all oscillators vibrating in phase. These two modes will hereafter be denoted the top and bottom modes, respectively.

When the stacking coupling $\varepsilon = 0$ we have to choose either to represent the variation of the linear spectrum as a function of the parameter μ or the curvature κ, with the other parameters fixed at non-zero values. It turns out that both possibilities give similar results. Figure 3 shows the dependence of the linear spectrum on κ. There are three key features. Firstly, there are localized modes that separate from the continuous spectrum. Secondly, the top and

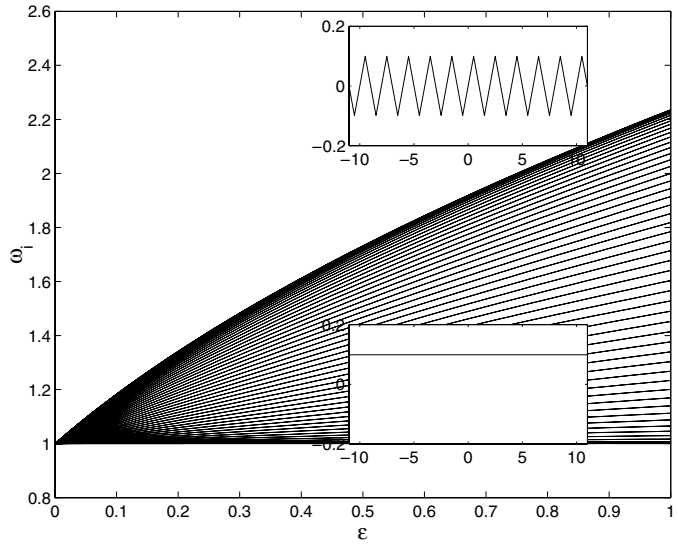

Figure 2. Dependence of the linear spectrum of the system on the stacking coupling parameter ε for a straight chain. The insets show the shape of the linear modes with highest and lowest frequencies.

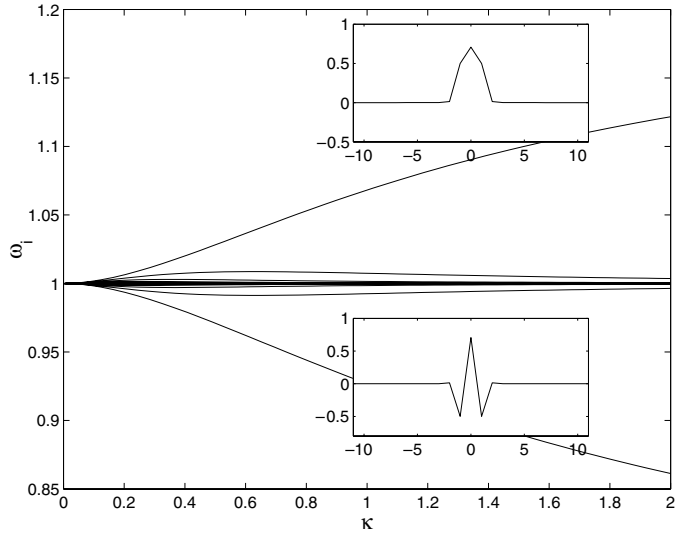

Figure 3. Dependence of the linear spectrum of the system on the curvature κ with stacking coupling parameter $\varepsilon = 0$ and dipole coupling parameter $\mu = 0.2$. The insets show the bell and zigzag shapes of the linear modes with highest and lowest frequencies, respectively.

bottom modes are localized within a radius of about a few units around the bending point and they become more localized as κ increases. Thirdly, the top mode has all the oscillators in phase, which we describe as being bell-shaped, while the bottom mode has neighbouring oscillators with opposite phase (zigzag-shaped). This change of profile is due to a change of

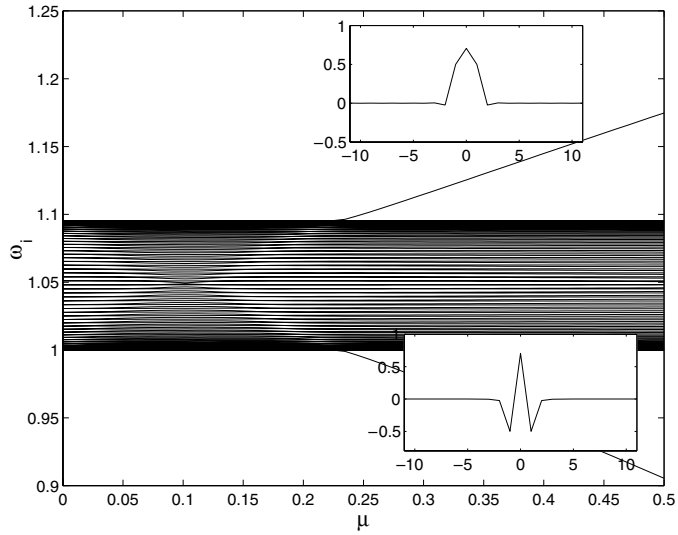

Figure 4. Dependence of the linear spectrum of the system on the dipole coupling parameter μ for constant stacking parameter $\varepsilon = 0.05$ and curvature $\kappa = 1$. The insets show the shape of the linear modes with highest and lowest frequencies, respectively.

the predominant coupling interaction when κ (or μ) is increased. Around the bending point, the sign in front of the variable u_m in the coupling terms of equation (3) changes from negative, i.e. attractive interaction, to positive, i.e. repulsive interaction. For homogeneous repulsive interaction, the linear spectrum would be as in figure 2, but with the frequencies spreading downwards and the zigzag mode at the bottom.

The localization does not depend on the number of sites in the system. If the dipole coupling parameter μ is changed at constant curvature κ, the spectrum is very similar with a slightly larger spread of the frequencies except for the top and bottom modes.

To conclude the description of the linear spectrum, we represent in figure 4 the dependence of the spectrum on the dipole parameter μ for a non-zero constant value of the stacking parameter $\varepsilon = 0.05$ and constant curvature $\kappa = 1$. It can be seen that for some value of μ the same localized modes separate from the continuous spectrum. Note that while studying breathers these modes are going to be those competing with nonlinear excitations and are predominant for high enough coupling. The frequency ω_b of the breathers has to be outside the continuous band or it will not be possible to obtain the breathers, which in physical terms means that the linear localized modes will resonate with the breather frequency and the energy will spread along the chain. If the on-site potential is hard, the breather frequency ω_b will be above the phonon band, $\omega_b > \omega_0$, therefore competing with the bell-shaped, top, linear mode. In the opposite case, $\omega_b < \omega_0$, the competing mode will be the zigzag-shaped, bottom mode. This is described in detail in the next section.

4. Hard breathers

To obtain breathers we need to choose the value of their frequency, which for a hard potential (here $V(u_n) = \frac{1}{2}\omega_0^2 u_n^2 + \frac{1}{4}u_n^4$) will be above $\omega_0 = 1$. Let us choose $\omega_b = 1.2$, i.e. a frequency not too far from the phonon band but outside it. The properties of the breathers with stacking

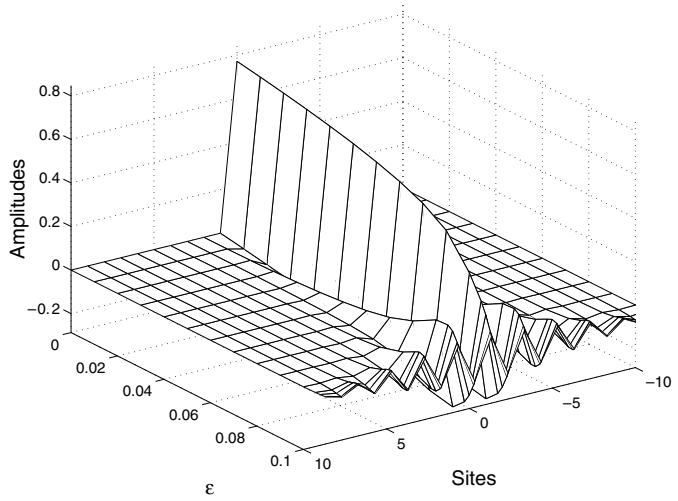

Figure 5. Dependence of the breather profile with hard on-site potential for the straight chain on the stacking parameter ε; frequency $\omega_b = 1.2$.

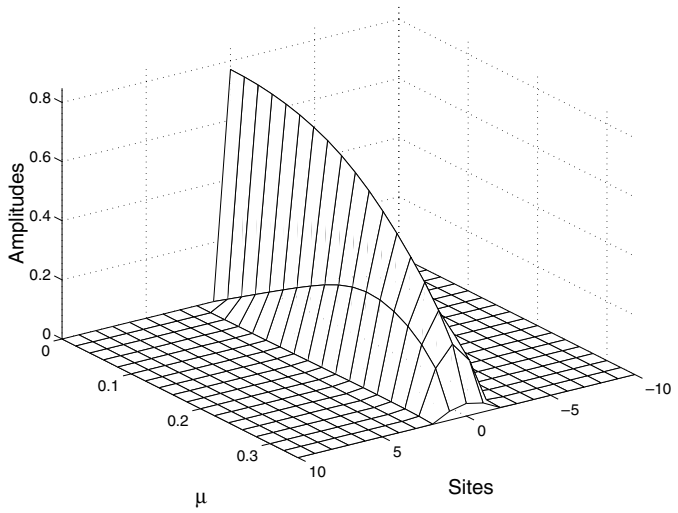

Figure 6. Dependence of the breather profile with hard on-site potential for a curved chain with curvature $\kappa = 2$ on the dipole coupling parameter μ with constant frequency $\omega_b = 1.2$; $\varepsilon = 0$.

coupling are well known, but we include them here for comparison. Figure 5 shows the profile of the breather while the parameter ε is changed. The path continuation using the Newton method finishes as the phonon band expands and collides with the breather frequency. The breather profile is a zigzag profile, which can also be easily deduced by tail analysis.

We obtain an analogous picture if the continuation is done with respect to the dipole coupling parameter μ, for constant curvature, until a bifurcation point. Now the breather obtains the bell profile shown in figure 6.

The fact that the breather amplitudes, i.e. $\{|u_n(0)|\} = \{\max_{\forall t}(|u_n(t)|)\}$, tend to zero is misleading. We are in the presence of an annihilation bifurcation [20], i.e. the Jacobian of

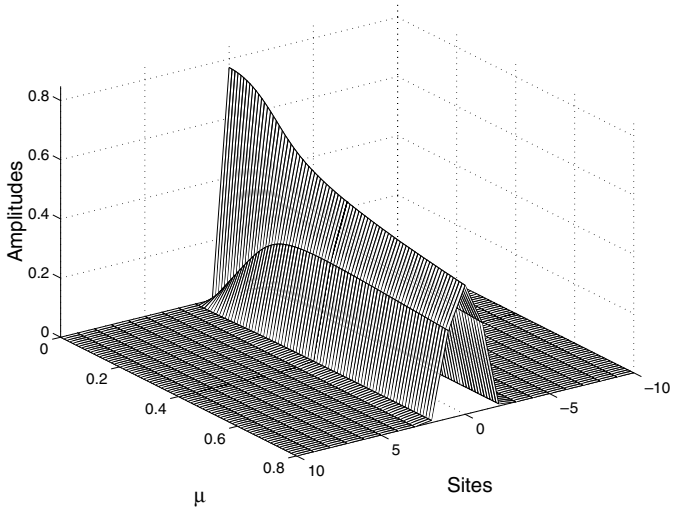

Figure 7. Dependence of the breather profile with hard on-site potential for a curved chain with curvature $\kappa = 2$ on the dipole coupling parameter μ for constant energy, $E = 0.3855$. The frequency changes from 1.2 to 1.46 and $\varepsilon = 0$.

the dynamical equation (3) with respect to $u = (u_1, u_2, \ldots, u_n)$ has an eigenvalue that tends to zero. This eigenvalue does not correspond to another breather in the neighbourhood of the parameter space but to the upper (for a hard potential) breather band [13] of the same breather. The physical meaning is that there are no localized excitations with the chosen frequency, except in the trivial case where the breather has zero amplitude, i.e. it is in the linear regime. We can obtain a complementary picture if the continuation is performed while keeping constant another characteristic of the breather. In [21] this is done with constant action. Here, using a similar technique, we have chosen to keep the energy constant, which is physically meaningful.

By fixing the energy, we restrict ourselves to the situation which is realized in single-molecule experiments. More biologically meaningful would be to keep constant not the energy but the temperature. This is, however, beyond the scope of our paper because to carry out this type of investigation it is necessary to introduce stochastic forces into the equations of motion and to solve the corresponding Langevin equations.

The dependence of the breather profile on the parameter μ at constant energy is plotted in figure 7. It can be seen that, by allowing the breather the freedom of choosing its frequency, the continuation is possible for much larger values of μ, or, in physical terms, there exist localized breathers although not at any frequency. Note that in this situation the phonon band is very narrow, and what we have is a nonlinear version of the linear mode described previously, whose frequency is close to the breather frequency although not identical.

Although the cases described above are interesting to understand the phenomena, the situation with more physical interest is the process of curving the chain. Suppose that $\varepsilon \neq 0$ and $\mu \neq 0$ and the breather has its frequency above the phonon band. When the chain is curved, the dependency of the breather with respect to the curvature is similar as with respect to μ. If we choose to keep the frequency constant, the plot of the breather evolution is very similar to figure 6, except for the fact that at the zero curvature the breather would have a zigzag profile which progressively changes to a bell profile for large enough curvature. Perhaps more interesting is the choice of keeping the energy constant, as it is a conserved quantity. The

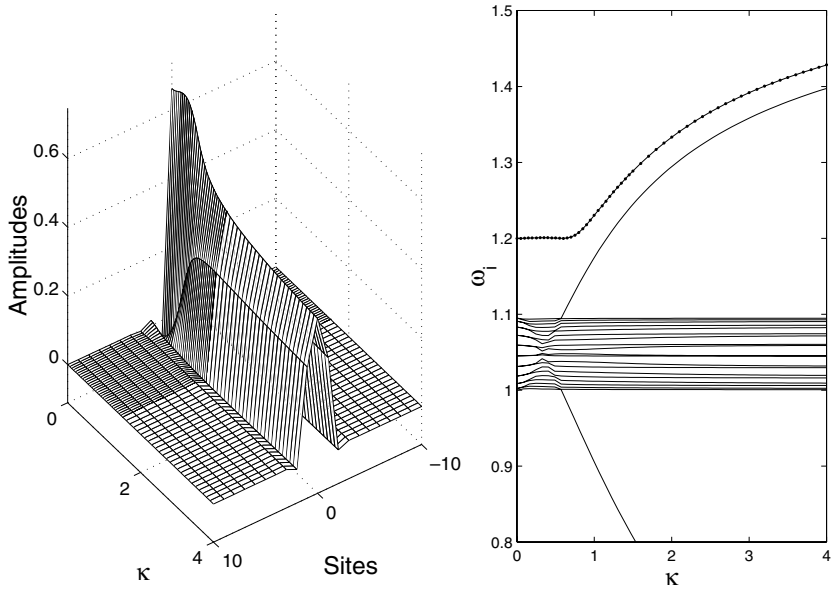

Figure 8. Left: dependence of the breather profile with hard on-site potential for a curved chain on the curvature at constant energy. Right: plot of the breather frequency (dots) and the linear spectrum with respect to the curvature. $E = 0.3064$, $\varepsilon = 0.05$ and $\mu = 0.5$.

dependence of the breather amplitudes and frequency are shown in figure 8. In the figure to the right we can see how the linear mode appears and the frequency of the top mode increases until almost colliding with the breather frequency. The breather with frequency $\omega_b = 1.2$ no longer exists while there exists a breather which is the nonlinear analogue of the top linear mode and its frequency increases as the chain is curved.

The linear mode is a solution of equation (3), with $\Psi = 0$, or, equivalently, with almost zero amplitudes for $\Psi \neq 0$. What we have called its nonlinear analogue is the solution of the same equation with $\Psi \neq 0$ having non-zero amplitudes and a similar profile, as shown in figure 8. It has more than a single harmonic in its linear spectrum. These extra harmonics are significantly larger for breathers with soft on-site potentials, as studied in the next section. In the case studied here, as the linear mode is localized, and, therefore, its frequency is isolated from the phonon band, the nonlinear analogue can be obtained by substituting $\Psi \to s\Psi$ in equation (3), and changing continuously s from zero to 1 at constant energy.

The observation of figure 8 shows that, for frequencies above the top of the phonon band, i.e. slightly below 1.1 for the parameters in the figure, it is only possible to continue the breather with the curvature at constant frequency until it approaches the top mode frequency curve. Thereafter, it is possible to continue it at constant energy, and its frequency follows slightly above the top mode.

If the chain is curved around the neighbouring site where the initial excitation is located, it will switch to the bending point, for even small curvature, when the frequency of the top linear mode approaches its frequency. This occurs at $\kappa = 0.7$ for the values corresponding to figure 8. Similar behaviour has been found in [6].

Let us mention that all the breathers described here are linearly stable, i.e. all their Floquet eigenvalues have modulus 1. The hard breathers in this system are always stable. The properties of the soft breathers are very different.

5. Soft breathers

We have included the previous section for completeness but, actually, in biological molecules chemical bonds are thought to be better described by soft potentials. The most commonly used are the quartic soft, $V(u_n) = \frac{1}{2}\omega_0^2 u_n^2 - \frac{1}{4}u_n^4$, the cubic potential, $V(u_n) = \frac{1}{2}\omega_0^2 u_n^2 - \frac{1}{3}u_n^3$, the Lennard–Jones potential, $V(u_n) = \sigma(1/r^6 - 1/r^{12})$, and the Morse potential $V(u_n) = D(\mathrm{e}^{-bu_n} - 1)^2$. The last two are known to have several good characteristics: (a) they are asymmetric, with a hard part, that describes the strong repulsion when two atoms or molecules approach, and a soft part that becomes flat, reflecting the weakening of the bond when the molecules get separated and eventually unbonded; (b) they have moving breathers with stacking coupling potentials; (c) compared with another frequently used soft potential, the cubic potential, they do not have an infinite well, which has no physical interpretation and can produce anomalous results when simulations are performed. To present our results, we have chosen the Morse potential because it is mathematically simpler, but the Lennard–Jones potential provides similar results.

For the straight chain and the normalized Morse potential $D = \frac{1}{2}$ and $b = 1$, which gives the same frequency $\omega_0 = 1$ for small oscillations, and a representative frequency of the nonlinear excitations $\omega_\mathrm{b} = 0.8$, the breathers are bell-shaped, their amplitudes grow with the coupling parameter and they become unstable for $\varepsilon = 0.12$. The nonlinear mode that produces the instability is a spatially asymmetric one. This will be of special interest in the section on moving breathers.

For stationary breathers, we are interested in values of the parameters where the dipole interaction is significant and the nonlinearity is weak. In this situation, typical parameters can be $\varepsilon = 0.05$ and $\mu = 0.5$. For these parameters, the frequencies of the phonon band, i.e. the continuous part of the linear spectrum, spread from 1 to 1.1. A rough measure of the nonlinearity of the excitation is the distance of its frequency from the phonon band, which suggest a frequency of around 0.8 or 0.9.

If we start with the straight chain and a breather centred at the bending point and we increase the curvature at constant frequency, the same difficulties as with the hard breathers arise; the amplitudes of the breathers tend to zero when its frequency approaches the bottom linear mode and the continuation becomes impossible. We must emphasize this point; in the literature on breathers, path continuation is usually carried out at constant frequency, which is a natural consequence of the theorems of existence [11] from the anti-continuous limit. At the anti-continuous limit, there exists freedom to choose the frequency of the isolated oscillators and therefore at low coupling too. This is not the case if the system is in the presence of strongly localized modes; there are no localized excitations at every frequency. This characteristic opens the possibility of spectroscopic analysis to check for the existence of breathers in biomolecules and eventually to measure curvatures.

From the mathematical point of view, if the frequency is not fixed, we need to fix another quantity, and the chosen one, as previously, is the energy. Thus, the variation of the breather with the curvature mimics an adiabatic process of bending. On the left, figure 9 shows the dependence of the breather profile with $\omega_\mathrm{b} = 0.8$ at $\kappa = 0$ on the curvature, changing its shape from a bell to a zigzag profile, until it becomes almost invariable. While this process takes place, its frequency changes, which is shown on the right of figure 9. The breather becomes unstable at $\kappa \approx 0.8$. The frequencies of another breather with lower energy and higher frequency are also represented in this figure. The higher the frequency, the larger the curvature, for which instability is produced.

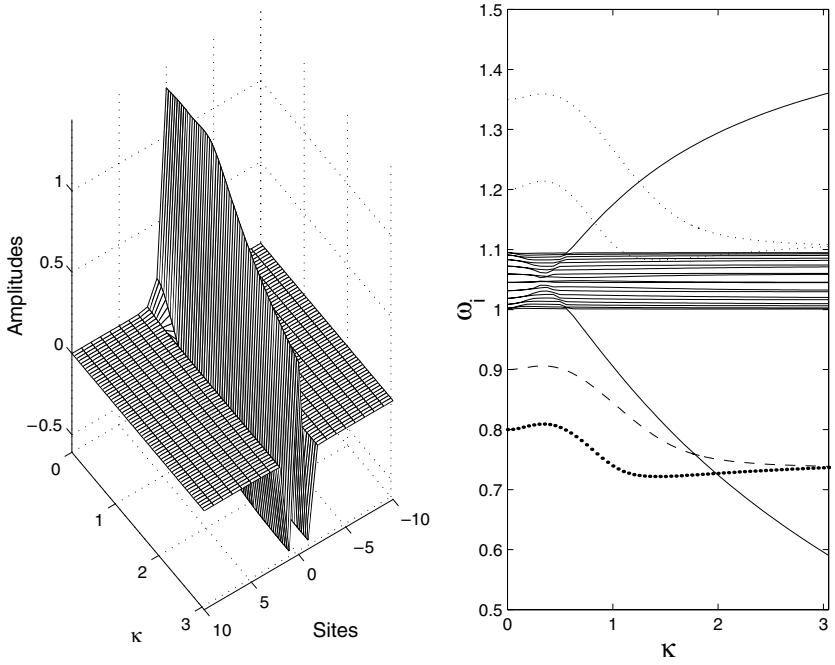

Figure 9. Left: dependence of the breather profile with soft on-site potential for a curved chain on the curvature at constant energy $E = 0.35$. Right: plot of the breather frequencies for two energies, $E = 0.35$ (large dots) and $E = 0.20$ (dashed curve), and 1.5 times the breather frequencies (small dots) and the linear spectrum (solid curves) with respect to the curvature. The parameters are $\varepsilon = 0.05$ and $\mu = 0.5$.

The exact stability analysis has been carried out by calculating the Floquet eigenvalues, but here we prefer to plot the breather frequency, the linear spectrum and 1.5 times the breather frequency. This gives a much more intuitive physical picture.

The reason for plotting this frequency is the following. When the curvature is increased, the frequencies $\{\omega_i\}$ of the internal modes, i.e. the small perturbation of the breather, are very similar to those shown in figure 4, as commented in section 3. The greatest difference is that the bottom mode with soft on-site potential (and the top mode for hard on-site potential) is not there, because this mode is substituted by the breather itself. The corresponding Floquet multipliers are $\{\lambda_i = \exp(\pm 2\pi\omega_i \mathrm{i}/\omega_\mathrm{b})\}$, $\{\theta_i = \pm 2\pi\omega_i/\omega_\mathrm{b}\}$ called the Floquet arguments. For an instability to be produced, a collision of two multipliers has to take place with the condition that they have the same Krein signature (see [13] for more detail on this subject). All of the positive (negative) Floquet arguments have the same positive (negative) signature and cannot therefore bring about instabilities until they collide at $(1+0i)$, called harmonic instabilities, or $(-1+0i)$, called subharmonic instabilities, or between them, called oscillatory instabilities or Krein crunches. The first occurs when $\theta_i = 2\pi n, n \in \mathbb{N}$, for some i, i.e. $\omega_i = n\omega_\mathrm{b}$, or in other words a linear mode resonates with the breather frequency or its harmonics. Figure 9 shows that this kind of bifurcation does not happen here.

The subharmonic instabilities can occur when $\theta_i = \pi + 2n\pi$, for some i, i.e. $\omega_i = \omega_\mathrm{b}/2 + n\omega_\mathrm{b}$. Within the range of parameters studied, this can only occur when some ω_i equals $1.5\omega_\mathrm{b}$. Therefore, subharmonic instabilities appear in our system, when some

frequency of the internal modes (very close to the linear modes, as commented above) collides with $1.5\omega_b$. This is easily seen by plotting simultaneously the $1.5\omega_b$ curve and the linear frequencies.

Figure 9 (right) shows the reason for this instability. The curve $1.5\omega_b$ intersects with the frequency curve of the top linear mode, bringing about the instability. Nevertheless, the latter is a localized mode, centred at the bending point and the localization persists although the excitation has now superimposed a perturbation with twice the breather period. Within the range of parameters shown, there are also Krein crunches, related with perturbations of the frequency, but also preserving the localization. This occurs after the Floquet multipliers of the phonon band have crossed at $(-1+0i)$, or, in other words, their frequencies have become larger than $1.5\omega_b$. The eigenvalues of the internal linear modes cross with other and do small excursions outside the unit circle. This is also evident as the curve $1.5\omega_b$ enters the phonon band. The same figure shows the frequency of a breather with higher energy corresponding to a frequency $\omega_b = 0.9$ at $\kappa = 0$. Note that both breathers tend to the same frequency as the curvature increases and that breathers with energy slightly below $E = 0.35$ avoid the secondary bifurcations, because the $1.5\omega_b$ curve does not intersect the phonon band.

The apparent intersection of the breather frequency with the bottom linear mode is misleading because the latter does not exist as a perturbation of the breather, this being its nonlinear analogue. The breather is not, however, linear, as its first ac harmonic is of the order of the dc one, and the second is about one-third of it.

6. Moving breathers

In this section, we explain briefly the behaviour of a moving breather in a curved region of the alpha–helix.

In order to move a breather, we apply the marginal mode method [17]. This basically consists of adding a spatially asymmetric mode (the pinning mode) to the breather velocity. As is shown in [20], the stacking coupling of the breather must be strong enough in order that it can be moved.

The scenario is similar to that observed in DNA chains [10] and biopolymers [4], i.e. for a fixed value of the curvature there exists a critical value of the velocity below which the breather is reflected when it reaches the bending point and, above which, the breather crosses through it. Analogously, for a fixed value of the velocity, the breather crosses the bending point as long as the curvature is smaller than a critical value. As the curvature increases, the breather spends more and more time at the bending point and is eventually reflected. These two behaviours are shown in figures 10 and 11. In other words, the moving breather in a curved alpha–helix chain behaves as a particle in a potential barrier.

In [22] a hypothesis is introduced about the existence of trapping in inhomogeneous Klein–Gordon lattices. According to this, the trapping of breathers does not occur when there exists a linear localized mode with a profile (vibration pattern or wave vector) different from the stationary breather one. When this occurs, the moving breather behaves as a particle in a potential barrier and is never trapped. As figure 4 shows, there is a localized mode (the top mode) of opposite profile to the breather, and the case exposed in the reference cited above is the same as in the curved alpha–helix. The simulations confirm that the trapping hypothesis [22] holds in our system, and moving breathers cannot be trapped.

We still have not been able to find a counterexample, and this hypothesis seems generic for Klein–Gordon systems. However, it has no mathematical proof and should be checked as much as possible to achieve, at least, an inductive confirmation.

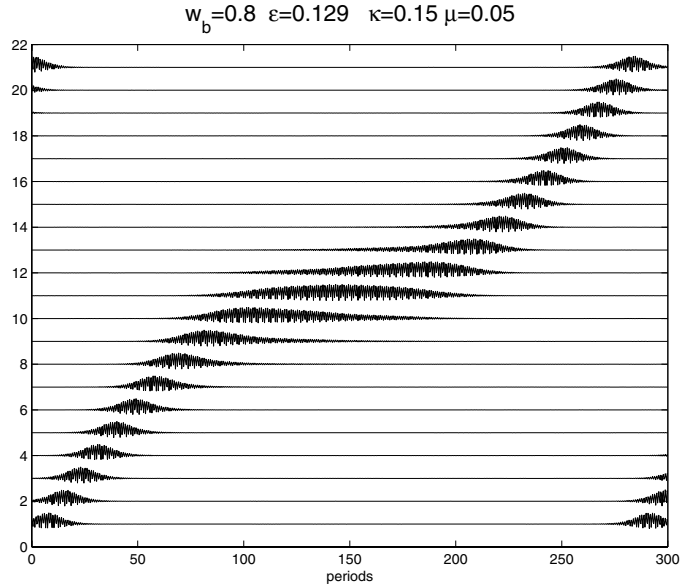

Figure 10. A breather travelling across the bending point. A small increase of the curvature will produce a reflection.

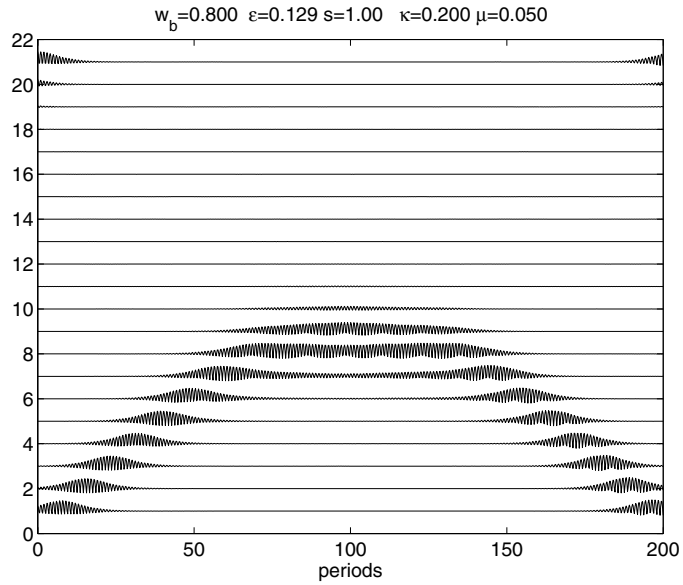

Figure 11. A breather being reflected at the bending point.

7. Conclusions

We have studied the existence and properties of stationary and moving breathers in a model with dipole moments parallel to a curved chain of oscillators. Its interest is twofold. On

the one hand, it is a model for a channel of amino acids along an alpha–helix protein, where the internal degrees of freedom are the amide-I vibrations. In this respect, the objective of our work is to explore the role of bending at places where the energy is stored and to investigate whether moving excitations can travel across a bending point or not. On the other hand, the theoretical interest comes from it being a model that completes previous works on bending chains. The specifics of the model are: (a) the dipoles are oriented along the chain instead of perpendicular to it; (b) it is sufficient to take into account nearest neighbours in order that the system can feel the shape of the chain.

In previous models [6, 7, 10, 20] the shape is felt due to the change between the distances of the oscillators and, therefore, they need long-range interaction in inextensible chains. In our model, the shape is felt due to the change of the angles between dipole moments. In this way, we expect to help to complete the study of systems in curved chains and to approach to a generalized description.

The most important general fact, overlooked in the literature on breathers to our knowledge, is that the presence of strongly localized models around the bending point has such decisive a role; the breathers cannot be chosen at any frequency when the curvature is increased. Their interaction with the linear localized modes brings about frequencies approximately determined, and dependent on the curvature.

Consequently, we have developed a variant of the existing techniques, described in appendix B to obtain breathers at constant energy. Therefore, the continuation of the breathers, when the curvature is increased, models an adiabatic process of bending. It would have been more biologically meaningful to model this process at constant temperature, but this is outside the scope of the techniques used in this paper, which are related more to single-molecule experiments.

The adiabatic process of curving the chain transforms the initial breather into a nonlinear analogue to the top or bottom linear mode according to the on-site potential. The corresponding linear mode, therefore, does not exist in the presence of the breather and cannot produce instabilities. The consequence is that hard breathers in the bent chain are stable and soft breathers experience subharmonic instabilities that conserve, however, the localization.

We also have shown that, up to relatively high curvatures, moving breathers can travel across the bending point spending some time at it. They cannot, however, be trapped, which confirms recent developments in the field [22].

The physical suggestion is that breathers may be a means of storage and transport of energy in proteins, due to and in spite of their complex structure in the space. Certainly, our model is a rough description of such a complex system, yet the main conclusion of the present and previous studies could be that the properties of breathers in different curved chains are quite common. We also think that they might provide a means to experimentally detect breathers at the bending points, showing absorbtion of characteristic frequencies and their harmonics, which depend on the curvature. We are, presently, in contact with experimental groups to explore its feasibility.

Acknowledgments

This work has been supported by the European Commission under the RTN project LOCNET, HPRN-CT-1999-00163. J F R Archilla and Yu B Gaididei acknowledge Informatics and Mathematical Modelling, Technical University of Denmark, for its hospitality.

Appendix A. Details of the model

As mentioned in section 1, we describe the position of each amino acid by a vector $\boldsymbol{r}_n$, where n is an index. The distance between amino acids is supposed to be a constant a, i.e. $a = |\boldsymbol{r}_{n+1} - \boldsymbol{r}_n|$. The direction of the dipole moments are given by unit vectors $\boldsymbol{t}_n = (\boldsymbol{r}_{n+1} - \boldsymbol{r}_n)/|\boldsymbol{r}_{n+1} - \boldsymbol{r}_n|$ and the moments themselves are given by $\boldsymbol{p}_n = p_n \boldsymbol{t}_n$.

The interaction energy between two neighbouring dipoles n and $n+1$ is given by

$$\begin{aligned} U_{n,n+1} &= \frac{\boldsymbol{p}_{n+1}\boldsymbol{p}_n}{|\boldsymbol{r}_{n+1} - \boldsymbol{r}_n|^3} - 3\frac{\boldsymbol{p}_n(\boldsymbol{r}_{n+1} - \boldsymbol{r}_n) \cdot \boldsymbol{p}_{n+1}(\boldsymbol{r}_{n+1} - \boldsymbol{r}_n)}{|\boldsymbol{r}_{n+1} - \boldsymbol{r}_n|^5} \\ &= p_{n+1}p_n \left(\frac{\boldsymbol{t}_n\boldsymbol{t}_{n+1}}{|\boldsymbol{r}_{n+1} - \boldsymbol{r}_n|^3} - 3\frac{\boldsymbol{t}_n(\boldsymbol{r}_{n+1} - \boldsymbol{r}_n) \cdot \boldsymbol{t}_{n+1}(\boldsymbol{r}_{n+1} - \boldsymbol{r}_n)}{|\boldsymbol{r}_{n+1} - \boldsymbol{r}_n|^5} \right) \\ &= p_{n+1}p_n \left(\frac{\boldsymbol{t}_n\boldsymbol{t}_{n+1}}{a^3} - 3a^2\frac{\boldsymbol{t}_n\boldsymbol{t}_n \cdot \boldsymbol{t}_{n+1}\boldsymbol{t}_n}{a^5} \right) \\ &= (p_{n+1}p_n/a^3)\,(-2\boldsymbol{t}_{n+1}\boldsymbol{t}_n) = (p_{n+1}p_n/a^3)((\boldsymbol{t}_{n+1} - \boldsymbol{t}_n)^2 - 2). \end{aligned} \tag{A.1}$$

Suppose that the equilibrium value of $p_n = p_0, \forall n$, then we can express its non-equilibrium value as $p_n = p_0 + qu_n$, where u_n represent the stretching from the equilibrium positions. Substitution into equation (A.1) leads to

$$U_{n,n+1} = U^0_{n,n+1} + U^1_{n,n+1} + \left(-2\frac{q^2}{a^3} + \frac{q^2}{a^3}(\boldsymbol{t}_{n+1} - \boldsymbol{t}_n)^2 \right) u_{n+1}u_n. \tag{A.2}$$

The first two terms in this equation represent constant and linear terms, therefore they will not appear in the Hamiltonian, as its first derivatives with respect to the variables u_n at equilibrium, i.e. $u_n = 0$ must be zero. We represent the remaining term by $H_{n,n+1}$.

Suppose that the Hamiltonian of the system is given by

$$H = \sum_n \frac{1}{2}\dot{u}_n^2 + \frac{1}{2}\alpha^2 u_n^2 + \Psi(u_n) + \frac{1}{2}K(u_{n+1} - u_n)^2 + H_{n,n+1} \tag{A.3}$$

where α and K are positive constants and $\Psi(u_n)$ is the nonlinear part of the on-site potential. Rearranging the terms, we obtain

$$\begin{aligned} H = \sum_n \frac{1}{2}\dot{u}_n^2 + \frac{1}{2}\left(\alpha^2 - 4\frac{q^2}{a^3}\right)u_n^2 + \Psi(u_n) + \frac{1}{2}\left(K + 2\frac{q^2}{a^3}\right)(u_{n+1} - u_n)^2 \\ + \frac{q^2}{a^3}(\boldsymbol{t}_{n+1} - \boldsymbol{t}_n)^2 u_{n+1}u_n. \end{aligned} \tag{A.4}$$

Thus, the Hamiltonian can be written as

$$H = \sum_n \frac{1}{2}\dot{u}_n^2 + \frac{1}{2}\omega_0^2 u_n^2 + \Psi(u_n) + \frac{1}{2}\varepsilon(u_{n+1} - u_n)^2 + \mu(\boldsymbol{t}_{n+1} - \boldsymbol{t}_n)^2 u_{n+1}u_n$$

with $\omega_0 = 1$, $\varepsilon = (K + 2q^2/a^3)/\alpha'^2$, $\mu = q^2/(a^3\alpha'^2)$, where $\alpha'^2 = \alpha^2 - 4q^2/a^3$, with the time rescaled $t \to \alpha' t$ and the redefinition of $\Psi(u_n) \to \Psi(u_n)/\alpha'^2$. The initial Hamiltonian has been also divided by α'^2.

We keep the term ω_0 in the formulae, in spite of it being 1, as a reference because its meaning is the frequency at very low amplitude when the oscillators are isolated.

The corresponding dynamical equations are

$$\ddot{u}_n + \omega_0^2 u_n + \Psi'(u_n) + \varepsilon(2u_n - u_{n+1} - u_n) + \mu((\boldsymbol{t}_{n+1} - \boldsymbol{t}_n)^2 u_{n+1} + (\boldsymbol{t}_{n-1} - \boldsymbol{t}_n)^2 u_{n-1}) = 0 \tag{A.5}$$

which are written in a simplified notation in equation (3).

Appendix B. Breathers with constant energy

To obtain breathers with constant energy, we use a variant of the method in the time Fourier space [12, 23]. First, we obtain breathers by path continuation at constant frequency from the anti-continuous limit using the Newton method, as described in the references above. Thereafter, the path continuation is performed at constant energy. In this case, our variant applies and we give below the details needed to obtain the corresponding Jacobian used by the Newton method. This is also a variant of the method developed in [21] at constant action.

The Hamiltonian of the system can be written:

$$H = \frac{1}{2}\sum_n \dot{u}_n^2 + W(u,\kappa) \tag{B.1}$$

where $u = (u_1, \ldots, u_N)$, $W(u,\kappa)$ represents the potential energy sum of the on-site and coupling energies, and κ represents any parameter—the curvature in this paper. The dynamical equations are given by $\ddot{u}_n + \frac{\partial W}{\partial u_n} = 0$. Time-reversible periodic solutions with frequency ω_b are given by a truncated Fourier series:

$$u_n(t) = \sum_{k=0}^{k_m}(2-\delta_{k,0})z_{k,n}\cos(k\omega_b t). \tag{B.2}$$

The use of functions with different frequencies is inconvenient and can be avoided by the change of variable $\tilde{t} = \omega_b t$, which leads to the Hamiltonian

$$H = \frac{1}{2}\omega_b^2\sum_n u_n'^2 + W(u,\kappa) \tag{B.3}$$

where $'$ represents the derivative with respect to $\tilde{t}$. The corresponding dynamical equations are

$$f_n(u,\omega_b,\kappa) \equiv \omega_b^2 u_n'' + \frac{\partial W}{\partial u_n} = 0. \tag{B.4}$$

In these equations, ω_b enters as a parameter and the functions u_n, with frequency unity in the new time variable, are given by

$$u_n(\tilde{t}) = \sum_{k=0}^{k_m}(2-\delta_{k,0})z_{k,n}\cos(k\tilde{t}). \tag{B.5}$$

Therefore, the functions f_n can be seen as 2π-periodic functions of $\tilde{t}$ due to their dependence on $u(\tilde{t})$ and $u''(\tilde{t})$.

The components of the cosine discrete Fourier transform of the dynamical equations (B.4) are given by

$$F_k[f_n] = -k^2\omega_b^2 z_{k,n} + F_k\left[\frac{\partial W}{\partial u_n}(u(\tilde{t}))\right] \tag{B.6}$$

where $F_k[g(\tilde{t})]$ represents the kth term in the cosine discrete Fourier transform of a 2π-periodic function $g(\tilde{t})$, given by

$$F_k[g(\tilde{t})] = \frac{1}{2k_m+1}\sum_{m=0}^{k_m}(2-\delta_{m,0})g\left(\frac{2\pi m}{2k_m+1}\right)\cos\left(\frac{2\pi km}{2k_m+1}\right). \tag{B.7}$$

In this way, finding a breather is reduced to solving the $(k_m+1)\times N$ equations (B.6). As a breather solution is determined by the same number of Fourier coefficients $z_{k,n}$ and the frequency ω_b, we need an extra equation. If we are interested in obtaining solutions with

given energy E, this is given by $H - E = 0$, which for time-reversible solutions ($u'_n(0) = 0$) reduces to

$$F_H \equiv W(u(0), \kappa) - E = 0.$$

We denote by $\tilde{z}$ and $\tilde{F}$ the column matrices ($\{z_{k,n}\}, \omega_b$) and ($\{F_k[f_n]\}, F_H$), respectively, with the index k running faster. In order to use the Newton method for path continuation with the parameter κ we need the Jacobian

$$\frac{\partial \tilde{F}}{\partial \tilde{z}} = \begin{bmatrix} \left[\left\{\frac{\partial F_k[f_n]}{\partial z_{k',n'}}\right\}\right] & \begin{matrix} \frac{\partial F_k[f_n]}{\partial \omega_b} \\ \vdots \end{matrix} \\ \left\{\frac{\partial F_H}{\partial z_{k',n'}}\right\} \quad \cdots & \frac{\partial F_H}{\partial \omega_b} \end{bmatrix}. \tag{B.8}$$

The left upper block is the Jacobian at constant frequency, and its elements are given by

$$\frac{\partial F_k[f_n]}{\partial z_{k',n'}} = -k^2\omega_b^2\delta_{k,k'}\delta_{n,n'} + \frac{2-\delta_{0,k'}}{2}\left(F_{k+k'}\left[\frac{\partial^2 W}{\partial u_n \partial u_{n'}}\right] + F_{|k-k'|}\left[\frac{\partial^2 W}{\partial u_n \partial u_{n'}}\right]\right). \tag{B.9}$$

The elements in the last column are given by

$$\frac{\partial F_k[f_n]}{\partial \omega_b} = -k^2\omega_b z_{k,n} \qquad \frac{\partial F_H}{\partial \omega_b} = \frac{\partial W(u(0))}{\partial \omega_b} = 0. \tag{B.10}$$

The remaining elements in the last row are

$$\begin{aligned} \frac{\partial F_H}{\partial z_{k',n'}} &= \frac{\partial W(\{u_n(0)\})}{\partial z_{k',n'}} = \frac{\partial W\left(\left\{\sum_{l=0}^{k_m}(2-\delta_{l,0})z_{l,m}\right\}\right)}{\partial z_{k',n'}} = \left(\frac{\partial W}{\partial u_{n'}}\right)_{t=0}(2-\delta_{k',0}) \\ &= -\ddot{u}_{n'}(0)(2-\delta_{k',0}) = \left(\sum_{l=0}^{k_m} l^2\omega_b^2 z_{l,n'}\right)(2-\delta_{k',0}). \end{aligned} \tag{B.11}$$

References

[1] Gaididei Y B, Mingaleev S F and Christiansen P L 2000 Curvature-induced symmetry breaking in nonlinear Schrodinger models *Phys. Rev.* E **62** R53–R56

[2] Christiansen P L, Gaididei Yu B and Mingaleev S F 2001 Effects on soliton dynamics in a chain of nonlinear oscillators *J. Phys.: Condens. Matter* **6** 1181–92

[3] Reigada R, Sancho J M, Ibañes M and Tsironis G P 2001 Resonant motion of discrete breathers in curved nonlinear chains *J. Phys. A: Math. Gen.* **34** 8465–75

[4] Ibañes M, Sancho J M and Tsironis G P 2002 Dynamical properties of discrete breathers in curved chains with first and second neighbors interaction *Phys. Rev.* E **65** 041902–14

[5] Tsironis G P, Ibañes M and Sancho J M 2002 Transport of localized vibrational energy in biopolymer models with rigidity *Europhys. Lett.* **57** 697–703

[6] Archilla J F R, Christiansen P L, Mingaleev S F and Gaididei Yu B 2001 Numerical study of breathers in a bent chain of oscillators with long range interaction *J. Phys. A: Math. Gen.* **34** 6363–73

[7] Archilla J F R, Christiansen P L and Gaididei Yu B 2002 Interplay of nonlinearity and geometry in a DNA-related, Klein–Gordon model with long-range dipole–dipole interaction *Phys. Rev.* E **65** 16609–16

[8] Ting J J L and Peyrard M 1996 Effective breather trapping mechanism for DNA transcription *Phys. Rev.* E **53** 1011–20

[9] Forinash K, Cretegny T and Peyrard M 1997 Local modes and localization in a multicomponent nonlinear lattice *Phys. Rev.* E **55** 4740–56

[10] Cuevas J, Palmero F, Archilla J F R and Romero F R 2002 Moving breathers in a bent DNA-related model *Phys. Lett.* A **299** 221–5

[11] MacKay R S and Aubry S 1994 Proof of existence of breathers for time-reversible or Hamiltonian networks of weakly coupled oscillators *Nonlinearity* **7** 1623–43

[12] Marín J L and Aubry S 1996 Breathers in nonlinear lattices: numerical calculation from the anticontinuous limit *Nonlinearity* **9** 1501–28
[13] Aubry S 1997 Breathers in nonlinear lattices: existence, linear stability and quantization *Physica* D **103** 201–50
[14] Flach S and Willis C R 1998 Discrete breathers *Phys. Rep.* **295** 181–264
[15] Binder P, Abraimov D and Ustinov A V 2000 Diversity of discrete breathers observed in a Josephson ladder *Phys. Rev.* E **62** 2858–62
[16] Trias E, Mazo J J and Orlando T P 2000 Discrete breathers in nonlinear lattices: experimental detection in a Josephson array *Phys. Rev. Lett.* **84** 741–4
[17] Aubry S, Chen D and Tsironis G 1996 Breather mobility in discrete ϕ^4 nonlinear lattices *Phys. Rev. Lett.* **77** 4776–9
[18] Aubry S and Cretegny T 1998 Mobility and reactivity of discrete breathers *Physica* D **119** 34–46
[19] Mackay R S and Sepulchre J-A 2002 Effective Hamiltonian for travelling discrete breathers *J. Phys. A: Math. Gen.* **35** 3985–4002
[20] Cuevas J, Archilla J F R, Gaididei Yu B and Romero F R 2002 Moving breathers in a DNA model with competing short and long range dispersive interactions *Physica* D **163** 106–26
[21] Archilla J F R, MacKay R S and Marín J L 1999 Discrete breathers and Anderson modes: two faces of the same phenomenon? *Physica* D **134** 406–18
[22] Cuevas J, Palmero F, Archilla J F R and Romero F R 2002 Moving discrete breathers in a Klein–Gordon chain with an impurity *Preprint* nlin.PS/0203026 To appear in *J. Phys. A: Math. Gen.*
[23] Marín J L 1997 Intrinsic Localised Modes in Nonlinear Lattices *PhD Dissertation* University of Zaragoza, Department of Condensed Matter